

1 ***In Silico* Identification and Experimental Validation of** 2 **Novel KPC-2 β -lactamase Inhibitors**

3 R. Klein^{[a,f]§}, P. Linciano^{[b]§}, G. Celenza^[c], P. Bellio^[c], S. Papaioannou^[b], J. Blazquez^[d], L. Cendron^[e],
4 R. Brenk^{[f]*} and D. Tondi^{[b]*}.

5

6 ^[a] Institute of Pharmacy and Biochemistry, Johannes Gutenberg University, Staudinger Weg 5, 55128
7 Mainz, Germany.

8 ^[b] Dipartimento di Scienze della Vita, Università di Modena e Reggio Emilia, Via Campi 103, 41125,
9 Modena, Italy.

10 ^[c] Dipartimento di Scienze Cliniche Applicate e Biotecnologie, Università dell'Aquila, Via Vetoio, 1,
11 67100 L'Aquila, Italy.

12 ^[d] Department of Microbial Biotechnology, National Center for Biotechnology, Consejo Superior de
13 Investigaciones Científicas (CSIC), C/ Darwin, 3, Campus de la Universidad Autonoma-Cantoblanco,
14 28049-Madrid, Spain

15 ^[e] Dipartimento di Biologia, Università di Padova, Viale G. Colombo 3, 35121, Padova, Italy.

16 ^[f] Department of Biomedicine, University of Bergen, Jonas Lies vei 91, 5020 Bergen, Norway

17 [§] Both authors contributed equally to this work.

18 * Corresponding authors. Email: tondi.donatella@unimore.it; Ruth.Brenk@uib.no

19

20

21 **Abstract**

22 Bacterial resistance has become a worldwide concern, particularly after the emergence of resistant
23 strains overproducing carbapenemases. Among these, the KPC-2 carbapenemase represents a significant
24 clinical challenge, being characterized by a broad substrate spectrum that includes aminothiazoleoxime
25 and cephalosporins such as cefotaxime. Moreover, strains harboring KPC-type β -lactamases are often
26 reported as resistant to available β -lactamase inhibitors (clavulanic acid, tazobactam and sulbactam).
27 Therefore, the identification of novel non β -lactam KPC-2 inhibitors is strongly necessary to maintain
28 treatment options. This study explored novel, non-covalent inhibitors active against KPC-2, as putative
29 hit candidates. We performed a structure-based *in silico* screening of commercially available compounds
30 for non- β -lactam KPC-2 inhibitors. Thirty-two commercially available high-scoring, fragment-like hits
31 were selected for *in vitro* validation and their activity and mechanism of action *vs* the target was
32 experimentally evaluated using recombinant KPC-2. N-(3-(1H-tetrazol-5-yl)phenyl)-3-
33 fluorobenzamide (**11a**), in light of its ligand efficiency (LE = 0.28 kcal/mol/non-hydrogen atom) and
34 chemistry, was selected as hit to be directed to chemical optimization to improve potency *vs* the enzyme
35 and explore structural requirement for inhibition in KPC-2 binding site. Further, the compounds were
36 evaluated against clinical strains overexpressing KPC-2 and the most promising compound reduced the
37 MIC of the β -lactam antibiotic meropenem by four fold.

38

39 Introduction

40 The emergence of KPC-2 class-A Beta-Lactamase (BL) carbapenemase, which confers resistance to last
41 resort carbapenems, poses a serious health threat to the public. KPC-2, a class A BL, uses a catalytic
42 serine to hydrolyze the β -lactam ring. Specifically, the hydrolysis reaction proceeds through a series of
43 steps involving: (i) the formation of a pre-covalent complex, (ii) the conversion to a high-energy
44 tetrahedral acylation intermediate, (iii) followed by a low-energy acyl-enzyme complex, (iv) a high-
45 energy tetrahedral de-acylation intermediate consequent to catalytic water attack, and (v) finally the
46 release of the hydrolyzed β -lactam ring product from the enzyme. [1–6].

47 Notably to treat infections caused by bacteria that produce class A BLs, mechanism-based inhibitors
48 (i.e., clavulanic acid, sulbactam, and tazobactam) are administered in combination with β -lactam
49 antibiotics. However, strains harboring KPC-type β -lactamases are reported to be resistant to available
50 β -lactamase inhibitors. Moreover, because of KPC-2's broad spectrum of activity (which includes
51 penicillins, cephalosporins, and carbapenems) treatment options against KPC-2-producing bacteria are
52 scarce, and “last-resort” carbapenems are ineffective as well [7]. Therefore, studies directed to the
53 discovery of novel, non β -lactam KPC-2 inhibitors have multiplied in the last years. Recently, new drugs
54 able to restore susceptibility to β -lactams i.e. the novel inhibitor avibactam in combination with
55 ceftazidime (CAZ) and RPX7009 (vaborbactam) with meropenem have been approved (Fig. 1)[8-10].

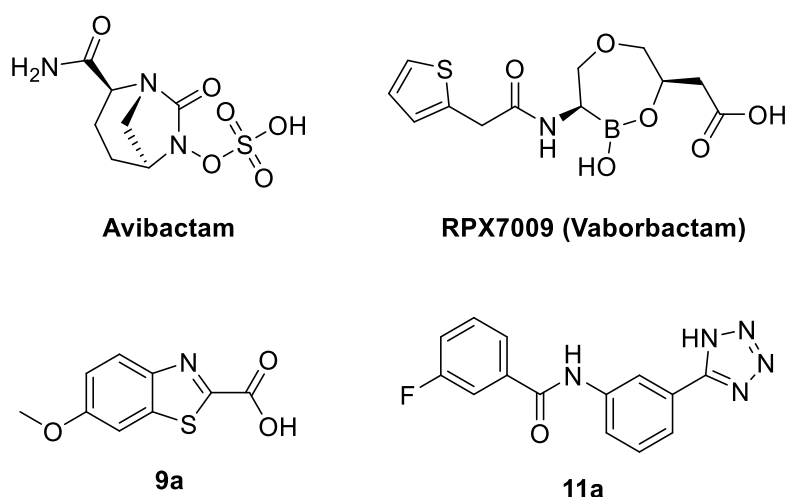


Figure 1. Chemical structure of avibactam, RPX7009, and compounds **9a** and **11a**

56 As attention on KPC-2 rises, the number of crystal structures of its apo and complexed form disclosed
57 in the PDB has increased, making KPC-2 a druggable target for structure based drug design efforts and
58 for the study of novel, non β -lactam like inhibitors of this threatening carbapenemase [9–12]
59 Recently, two crystal structures of the hydrolyzed β -lactam antibiotics cefotaxime and faropenem in
60 complex with KPC-2 were determined (PDB codes 5UJ3, 5UJ4; Fig. 2).[13]

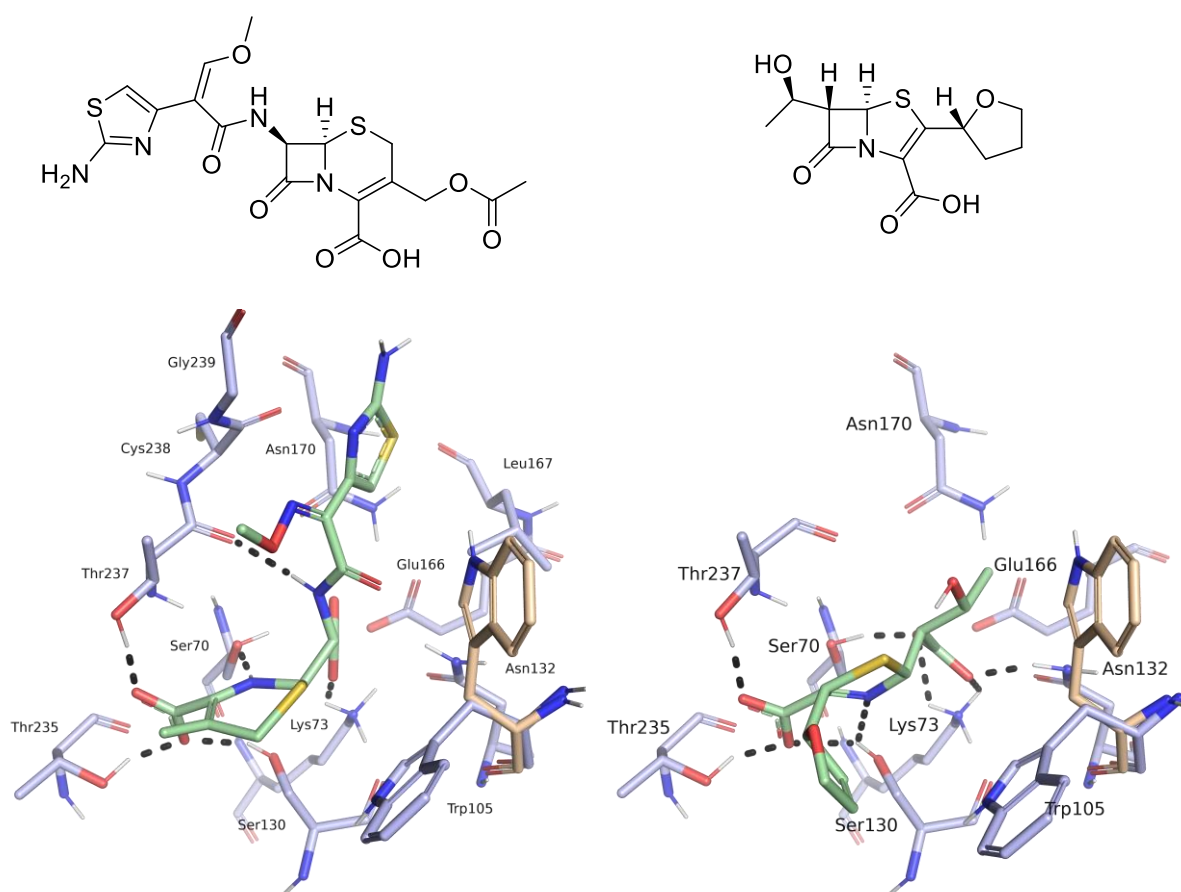


Figure 2. Structures and binding modes of hydrolyzed β -lactam antibiotics in the KPC-2 binding site. Left: binding mode of hydrolyzed cefotaxime (PDB code 5UJ3). Right: binding mode of hydrolyzed faropenem (PDB code 5UJ4). The second rotamer of Trp105 adopted in the apo-enzyme is coloured in beige, protein side chains in blue and ligands in green. Hydrogen bonds are indicated as black dots.

62 Both ligands form hydrogen-bond interactions with their C4-carboxyl group to Ser130, Thr235 and
63 Thr237. The dihydrothiazine moiety of cefotaxime and the dihydrothiazole moiety of faropenem forms
64 π - π -stacking interactions with Trp105. In the apo-enzyme, this side chain adopts two rotamers, upon
65 binding of a ligand just one. Mutagenesis studies have shown the importance of Trp105 in substrate
66 recognition [7]. The faropenem ring nitrogen forms a hydrogen-bond interaction with Ser130, whereas
67 the ring nitrogen of cefotaxime a hydrogen bond with Ser70. The aminothiazole ring of cefotaxime
68 forms van-der-Waals contacts with Leu167, Asn170, Cys238 and Gly239, while the oxyimino group
69 and the hydroxyethyl group of faropenem are solvent exposed (Fig. 2).[13]

70 Based on this and other structural information, we used a hierarchical screening cascade for the
71 discovery of non β -lactam like KPC-2 inhibitors. The selected candidates were then validated as hits
72 against isolated recombinant KPC-2. Among the tested compounds **9a**, a benzotiazole derivative, and
73 **11a**, a tetrazole-containing inhibitor, showed the highest activity against KPC-2 and behaved as
74 competitive inhibitors of the targeted carbapenemase (Fig. 1). Compound **11a** was subsequently directed
75 to chemical optimization to improve potency *vs* the enzyme and explore structural requirement for
76 inhibition in KPC-2 binding site. Further, the compounds were evaluated against clinical strains
77 overexpressing KPC-2 and the most promising compound reduced the MIC of the β -lactam antibiotic
78 meropenem by four fold.

79

80 **Materials and Methods**

81 **Pharmacophore hypothesis**

82 A search for similar binding sites of KPC-2 was carried out using the online tool PoSSuM - Search K
83 [15,16]. Based on shared ligand interactions in the retrieved structures (Table 1), a pharmacophore was
84 defined based on a *K. pneumoniae* KPC-2 protein structure (PDB code 3RXW) [17] and the ligand OJ6
85 of CTX-M-9 β -lactamase (PDB code 4DE1) [18]. The derived pharmacophore contained a hydrogen-

86 bond acceptor feature for interaction with Thr237, Thr235 and Ser130, a hydrophobic feature for π -
87 stacking with Trp105 and a hydrogen bond acceptor feature for interactions with Asn132 (Fig. 3).

88

89

90 **Table 1:** Result of PoSSuM Search K for similar binding sites. Structures with binding sites similar
91 with structure 3RXW in complex with a non-covalent ligand were reported.

	PDB-code	Protein name	Resolution	Ref.
1	4BD0	<i>E.coli</i> β -lactamase TOHO-1	1.21 Å	[19]
2	3G30	<i>E.coli</i> β -lactamase CTX-M-9a	1.8 Å	[20]
3	4DE1	<i>E.coli</i> β -lactamase CTX-M-9a	1.26 Å	[18]
4	4DDY	<i>E.coli</i> β -lactamase CTX-M-9a	1.36 Å	[18]
5	4DE3	<i>E.coli</i> β -lactamase CTX-M-9a	1.44 Å	[18]
6	4DDS	<i>E.coli</i> β -lactamase CTX-M-9a	1.36 Å	[18]
7	4DE0	<i>E.coli</i> β -lactamase CTX-M-9a	1.12 Å	[18]
8	4EUZ	<i>S.fonticola</i> β -lactamase SFC-1	1.08 Å	[21]
9	4DE2	<i>E.coli</i> β -lactamase CTX-M-9a	1.40 Å	[18]
10	3G35	<i>E.coli</i> β -lactamase CTX-M-9a	1.41 Å	[20]
11	3G32	<i>E.coli</i> β -lactamase CTX-M-9a	1.31 Å	[20]
12	3G2Y	<i>E.coli</i> β -lactamase CTX-M-9a	1.31 Å	[20]
13	3G31	<i>E.coli</i> β -lactamase CTX-M-9a	1.70 Å	[20]

92

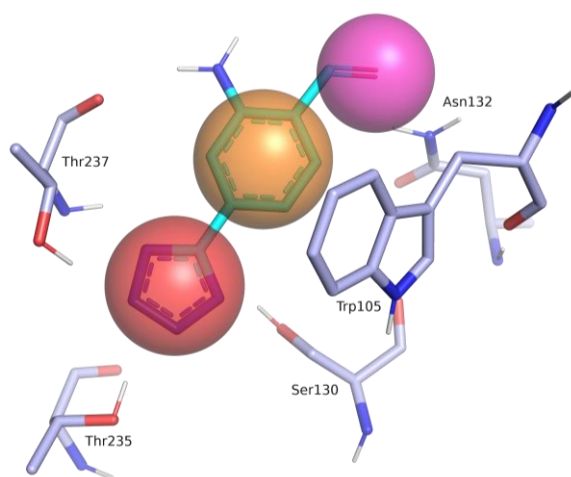


Figure 3. Binding site of KPC2 (PDB code 3RXW, blue) superimposed with a fragment of the ligand OJ6 bound to CTX-M-9 β -lactamase (PDB code 4DE1, cyan) and pharmacophore features (red:

hydrogen-bond acceptor, orange: hydrophobic interaction feature, purple: hydrogen-bond donor)
(Ambler numbering) [22].

93 **Virtual Screening**

94 Our in-house MySQL-database of commercially available compounds was filtered for compounds
95 fulfilling the following lead-like criteria: between 10 ten and 25 twenty-five heavy atoms, between one
96 and six hydrogen-bond acceptors, between one and three hydrogen-bond donors and a clog P between -
97 3 and 3. In addition, the complexity was limited by only including compounds with less than 7 rotatable
98 bonds and between 1 and 3 ring systems. Compounds containing unwanted reactive or toxic functional
99 groups were excluded as well [23].

100 In-house python scripts based on OpenEye's OEChem toolkit (OEChem, version 2016.6.1, OpenEye
101 Scientific Software, Inc., Santa Fe, NM, USA) were used to charge, tautomerize and stereoisomerize
102 the selected compounds. Conformers were generated using OpenEye's OMEGA toolkit [24]. The
103 pharmacophore filtering was carried out using Molecular Operating Environment (MOE, Chemical
104 Computing Group). Compounds that passed the pharmacophore filter were transformed into a format
105 suitable for docking as described previously [25].

106 The crystal structure of *K. pneumoniae* KPC-2 (PDB code 3RXW) [17] was used as receptor for
107 docking. The 'protonate 3D' tool of MOE was used to add polar hydrogen atoms to the receptor, energy
108 minimize their positions and to assign partial charges based on the AMBER force field parameters.
109 Water molecules and ligands (CIT and SR3) were deleted and the position of the Ser69 side chain was
110 energy minimized with the same force field parameters. The structure was aligned with the crystal
111 structure of *E.coli* CTX-M-9 (PDB code 4DE1) and the ligand 0J6 was used to define spheres as
112 matching points for docking. Grid-based excluded volume, van-der-Waals potential and electrostatic
113 potential as well as solvent occlusion maps were calculated as described earlier [26,27].

114 The compounds were docked into the binding site of KPC-2 using DOCK3.6 [27–29]. Parameters for
115 sampling ligand orientations were set as follows: bin size of ligand and receptor were set to 0.4 Å,
116 overlap bins were set to 0.2 Å and the distance tolerance for receptor and ligand matching spheres was

117 set to 1.5 Å. Each docking pose which did not overlap with the receptor was scored for electrostatic and
118 van-der-Waals complementarity and penalized according to its estimated partial desolvation energy. For
119 each compound, only the best-scoring pose out of its tautomers, protonation states or ring alignments
120 was saved in the final docking hit list. The docking hit list was filtered with the pharmacophore described
121 above, keeping the ligand positions rigid. Compounds passing this filter were ranked by their calculated
122 ligand efficiency [30,31] and inspected by eye.

123

124 **Expression and purification of recombinant KPC-2.**

125 The *bla*_{KPC-2} gene was kindly provided by Prof. Sergei Vakulenko (University of Notre Dame du Lac,
126 Indiana, USA) and cloned as already reported [32] and transformed into competent *E.coli* BL21 (DE3)
127 cells for protein expression. 50 mL of Tryptic Soy Broth (TSB) (50 mg/L kanamycin) were inoculated
128 with fresh colonies and grown at 37°C. 4 mL of the overnight culture was used to inoculate 1.3 L of
129 TSB (50 mg/L kanamycin) grown at 37°C with shaking to an optical density of 0.5 measured at 600 nm.
130 Then expression of recombinant *bla* gene was induced by adding 1.0 mM IPTG (isopropyl-D-
131 thiogalactopyranoside) and the cells were again allowed to grow at 20 °C overnight. Bacteria were
132 harvested by centrifugation at 4000 rpm for 20 minutes. The pelleted cells were resuspended in Tris-
133 HCl 50 mM pH 7.4-7.5. Periplasmatic proteins were extracted as reported in the pET System Manual
134 (TB055 10th Edition Rev. B 0403) and subsequently dialyzed in sodium acetate buffer (50 mM, pH
135 5.0). The protein was conveniently purified in a single step using a Macro-Prep High S resin and eluted
136 using sodium acetate 50 mM pH 5.0 and a sodium chloride (NaCl) linear gradient from 100 to 500 mM.
137 The purified protein was dialyzed overnight in sodium phosphate buffer 50 mM, pH 7.0 [32,33].

138

139 **Inhibition Assays**

140 The hydrolytic activity of KPC-2 activity was measured using the β-lactam substrates CENTA (100 uM,
141 K_M 70 uM) or nitrocefin (114 uM, K_M 36 μM) in reaction buffer consisting of 50 mM of PB at pH 7.0
142 at 25°C with 0.01% v/v Triton X-100 to avoid compound aggregation and promiscuous inhibition.[34]

143 Reactions were monitored using a Beckmann DU640® spectrophotometer at 405nm for CENTA and
144 480 nm wavelength for nitrocefin [35]. The test compounds were synthesized as described below or
145 purchased from Enamine, TimTec, Vitas-M, ChemBridge, Otava, Life Chemicals or Apollo Scientific
146 and assayed without further purification. Compounds were dissolved in dimethyl sulfoxide (DMSO) to
147 a concentration of 25 mM and stored at -20°C. The highest concentration at which the compounds were
148 tested was up to 1 mM (depending on their solubility). All experiments were performed in duplicate and
149 the error never exceeded 5%. The reaction was typically initiated by adding KPC-2 to the reaction buffer
150 last. To control for incubation effects, protein was added to the reaction buffer first, and the reaction
151 was initiated by the addition of reporter substrate after 10 minutes of enzyme-compound incubation.
152 The results are reported in Tables 2 and Table 3.

153 Competitive inhibition mechanism and the K_i for compound **9a** was determined by Lineweaver–Burk
154 (LB) and Dixon plots. For compound **11a**, already reported as competitive inhibitor of the extended
155 spectrum β -lactamase (ESBL) CTX-M15, the K_i was calculated by the Cheng-Prusoff equation ($K_i =$
156 $IC_{50}/(1 + [S]/K_M)$ assuming competitive inhibition [36].

157

158 **Synthetic procedures**

159 All commercially available chemicals and solvents were reagent grade and were used without further
160 purification unless otherwise specified. Reactions were monitored by thin-layer chromatography on
161 silica gel plates (60F-254, E. Merck) and visualized with UV light, cerium ammonium sulfate or alkaline
162 $KMnO_4$ aqueous solution. The following solvents and reagents have been abbreviated: ethyl ether
163 (Et_2O), dimethyl sulfoxide (DMSO), ethyl acetate ($EtOAc$), dichloromethane (DCM), methanol
164 (MeOH). All reactions were carried out with standard techniques. NMR spectra were recorded on a
165 Bruker 400 spectrometer with 1H at 400.134 MHz and ^{13}C at 100.62 MHz. Proton chemical shifts were
166 referenced to the TMS internal standard. Chemical shifts are reported in parts per million (ppm, δ units).
167 Coupling constants are reported in units of Hertz (Hz). Splitting patterns are designed as s, singlet; d,
168 doublet; t, triplet; q quartet; dd, double doublet; m, multiplet; b, broad. Mass spectra were obtained on
169 a 6520 Accurate-Mass Q-TOF LC/MS and 6310A Ion TrapLC-MS(n).

170

171 **General procedure for the synthesis of sulfonamides 1-6b**

172 To a solution of 3-(1H-tetrazol-5-yl)aniline (1 eq.) in DCM dry (25 mL) at room temperature and under
173 nitrogen atmosphere, pyridine (3 eq.) and the appropriate sulfonyl-chloride (1.2 eq.) were added. The
174 mixture was reacted at room temperature for 2-12 h. The reaction was quenched with aqueous saturated
175 solution of NH₄Cl and acidified at pH 4 with aqueous 1N HCl. The aqueous phase was extracted with
176 AcOEt, and the organic phase washed with brine, dried over Na₂SO₄ and concentrated. The crude was
177 crystalized from MeOH or Et₂O to give the desired product.

178 **N-(3-(1H-tetrazol-5-yl)phenyl)-3-fluorobenzenesulfonamide (1b)**

179 Pale yellow solid (150 mg, yield 47%). ¹H NMR (400 MHz, DMSO-d₆) δ 7.19 (dd, *J* = 2.2, 8.1 Hz,
180 1H), 7.33 – 7.45 (m, 2H), 7.47 – 7.58 (m, 3H), 7.62 (d, *J* = 7.7 Hz, 1H), 7.76 (t, *J* = 1.8 Hz, 1H), 10.61
181 (s, 1H), the H of tetrazole exchanges. MS *m/z* [M+H]⁺ 320.1; [M-1]⁻ 318.0.

182 **N-(3-(1H-tetrazol-5-yl)phenyl)-3-nitrobenzenesulfonamide (2b)**

183 Pink solid (62% yield). ¹H-NMR (400 MHz, DMSO-d₆) δ: 7.31 (ddd, *J* = 1.0, 2.3, 8.2 Hz, 1H), 7.51 (t,
184 *J* = 8.0 Hz, 1H), 7.74 (dt, *J* = 1.2, 7.8 Hz, 1H), 7.82 – 7.96 (m, 2H), 8.18 (dt, *J* = 1.3, 7.9 Hz, 1H), 8.46
185 (ddd, *J* = 1.0, 2.3, 8.2 Hz, 1H), 8.54 (t, *J* = 2.0 Hz, 1H), 10.90 (s, 1H); the H of tetrazole exchanges. ¹³C-
186 NMR (DMSO-d₆) δ: 117.35, 120.09, 123.04, 127.35, 129.17, 129.22, 129.69, 133.21, 136.59, 137.99,
187 139.81, 148.82, 154.28. MS *m/z* [M+H]⁺ Calcd for C₁₃H₁₀N₆O₄S: 346.0 Found: 347.2.

188 **N-(3-(1H-tetrazol-5-yl)phenyl)-5-(dimethylamino)naphthalene-1-**

189 **sulfonamide (3b)**

190 White solid (31% yield). ¹H NMR (400 MHz, DMSO-d₆) δ 2.78 (s, 6H), 7.20 (dd, *J* = 1.5, 7.6 Hz, 1H),
191 7.24 – 7.38 (m, 3H), 7.39 – 7.65 (m, 3H), 8.27 (dd, *J* = 1.6, 7.5 Hz, 1H), 8.41 (ddd, *J* = 1.5, 7.5, 19.3
192 Hz, 2H), the H of tetrazole exchanges. MS *m/z* [M+H]⁺ Calcd for C₁₉H₁₈N₆O₂S: 394.1 Found: 395.1.

193 **N-(4-(N-(3-(1H-tetrazol-5-yl)phenyl)sulfamoyl)phenyl)acetamide (4b)**

194 Pink solid (52% yield). ¹H NMR (400 MHz, DMSO-d₆) δ 2.12 (s, 3H), 7.31 (ddd, *J* = 1.0, 2.3, 8.2 Hz,
195 1H), 7.44 (t, *J* = 7.9 Hz, 1H), 7.65 – 7.72 (m, 3H), 7.74 – 7.79 (m, 2H), 7.86 (t, *J* = 1.9 Hz, 1H), the H
196 of tetrazole exchanges. ¹³C NMR (100 MHz, DMSO-d₆) δ 22.58, 118.86, 118.95, 122.60, 123.07,

197 126.32, 127.96, 128.87, 129.96, 133.69, 139.01, 142.97, 170.57. MS m/z [M+H]⁺ Calcd for
198 C₁₅H₁₄N₆O₃S: 358.1 Found: 359.2.

199 **N-(3-(1H-tetrazol-5-yl)phenyl)quinoline-8-sulfonamide (5b)**

200 White solid (88% yield). ¹H NMR (400 MHz, Acetone-d₆) δ 7.28 – 7.42 (m, 2H), 7.59 – 7.90 (m, 4H),
201 8.03 (dt, J = 1.1, 1.8 Hz, 1H), 8.25 (dd, J = 1.5, 8.2 Hz, 1H), 8.42 (dd, J = 1.4, 7.3 Hz, 1H), 8.52 (dd, J
202 = 1.8, 8.4 Hz, 1H), 9.21 (dd, J = 1.8, 4.3 Hz, 1H), 9.41 (s, 1H), the H of tetrazole exchanges. ¹³C NMR
203 (100 MHz, Acetone-d₆) δ 117.35, 120.09, 123.01, 123.04, 125.55, 128.06, 129.17, 129.69, 129.79,
204 130.11, 133.27, 139.81, 140.02, 140.84, 149.72, 154.28. MS m/z [M+H]⁺ Calcd for C₁₆H₁₂N₆O₂S: 352.1
205 Found: 353.2.

206 **N-(3-(1H-tetrazol-5-yl)phenyl)-4-chlorobenzenesulfonamide (6b)**

207 Light yellow solid (93% yield). ¹H NMR (400 MHz, Methanol-d₄) δ 7.57 (t, J = 8.0 Hz, 1H), 7.74 (dt,
208 J = 1.3, 7.9 Hz, 2H), 7.78 – 7.84 (m, 1H), 7.99 (d, J = 8.6 Hz, 2H), 8.06 (d, J = 8.6 Hz, 2H), 8.41 (t, J =
209 1.9 Hz, 1H), the H of tetrazole exchanges. ¹³C NMR (100 MHz, Methanol-d₄) δ 117.35, 120.09, 123.01,
210 123.04, 125.55, 128.06, 129.17, 129.69, 129.79, 130.11, 133.27, 139.81, 140.02, 140.84, 149.72,
211 154.28. MS m/z [M+H]⁺ Calcd for C₁₃H₁₀ClN₅O₂S: 335.0, 337.0 Found: 336.1, 338.2.

212

213 **Results and Discussion**

214 **Virtual Screening**

215 The binding sites in the available KPC-2 crystal structures were analyzed to select a suitable receptor
216 for docking. Alignment and superposition of the binding site residues of the seven available crystal
217 structures of *E.coli* and *K. pneumoniae* KpKPC-2 revealed a rather rigid binding site with only Trp105
218 adopting two different rotamers, a closed conformation found 6-times and an open one, found two-
219 times. In one structure, both rotamers were present (Fig.4). Thus, for virtual screening, the structure with
220 the highest resolution was selected (*K. pneumoniae* KPC-2 in complex with the covalent inhibitor
221 penamsulfone PSR-3-226 (PDB code 3RXW), 1.26 Å resolution). This structure contained both
222 rotamers of Trp105. For virtual screening, the closed conformation was chosen, as this is the most
223 dominant conformation upon ligand binding.

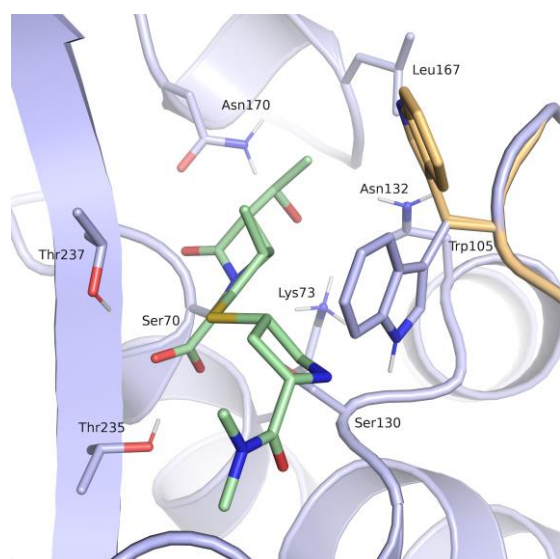


Figure 4. Binding site of *KpKPC2* (PDB code 3RXW) with ligand meropenem (green, PDB code 4EUZ). The receptor conformation used for docking is coloured in blue, the rotamer of Trp105 not considered in the docking setup in beige (Ambler numbering) [22].

224

225 Only little diversity with respect to bound ligands was found in the *KpKPC2* structures. To obtain a
226 more detailed picture on key interactions and to derive a pharmacophore hypothesis, PoSSuM - Search
227 K was used to search for similar binding sites containing non-covalent ligands. This resulted in thirteen
228 structures (Table 1), all having tetrazoles or carboxylates derivatives bound in the hydrophilic pocket
229 formed by the amino acids corresponding to Thr235, Thr237, Ser130 and Ser70 in *KpKPC2* (Fig.4).
230 Seven of the contained ligands were fragment hits for *E.coli* CTX-M class A extended spectrum β -
231 lactamase (ESBL), and four were derivatives of the most potent screening hit. Further, a structure of *S.*
232 *fonticola* SFC-1 S70A β -lactamase in a non-covalent complex with meropenem and one of *E.coli* Toho-
233 1 R274N: R276N β -lactamase in complex with a boronic acid were retrieved. Superposition of the
234 binding site residues of *KpKPC2* (PDB code 3RXW) and the CTX-M β -lactamase structures gave rmsd
235 values for the C α atoms between 0.72 and 0.82 Å, for superposition of *KpKPC2* and *S. fonticola* SFC-
236 1 (PDB code 4EUZ) 0.28 Å and for superposition *KpKPC2* and *E.coli* Toho-1 (PDB code 4BD0) 0.73
237 Å (Fig. 5).

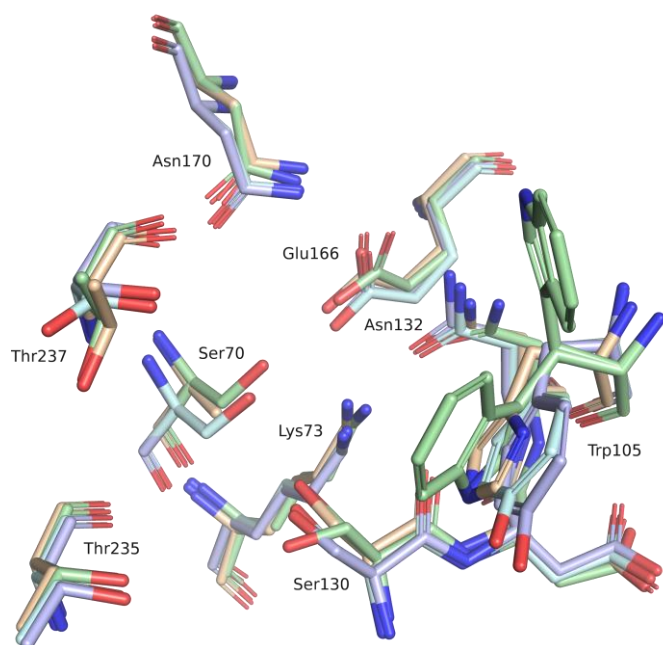


Figure 5. Superposition of the *Kp*KPC-2 binding site residues (PDB code 3RXW, green) with the *E.coli* CTX-M-9 β -lactamase (PDB code 4DDS, blue), the *S.fonticola* SFC-1 β -lactamase (PDB code 4EUZ, beige) and the *E.coli* TOHO-1 β -lactamase (PDB code 4BD0, cyan) (Ambler numbering) [22].

238

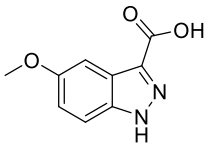
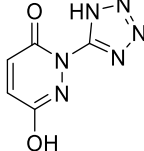
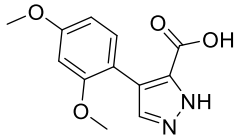
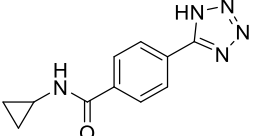
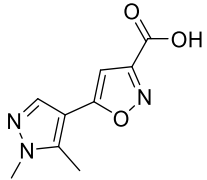
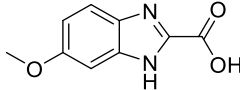
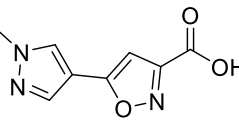
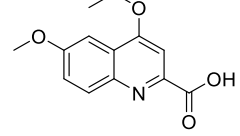
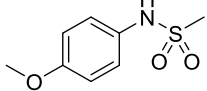
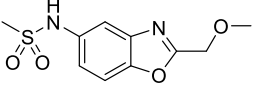
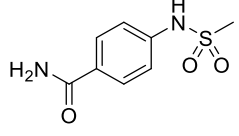
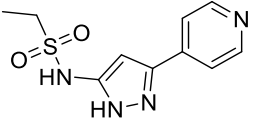
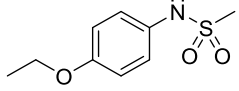
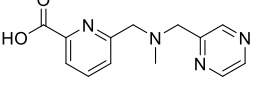
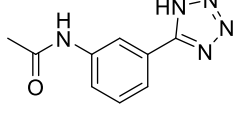
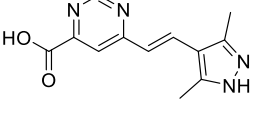
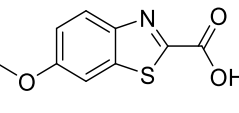
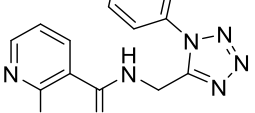
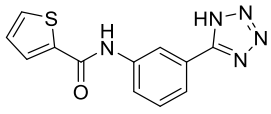
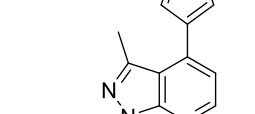
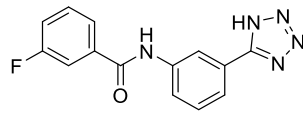
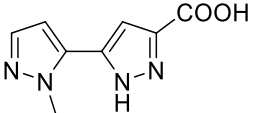
239 Based on the retrieved structures, a pharmacophore hypothesis was derived. All of the ligands in these
240 structures as well as the β -lactamase binding protein (PDB code 3E2L, 3E2K) and the covalent ligand
241 of the structure used as receptor, formed a hydrogen-bond with Thr235 or Thr237. Accordingly, a
242 hydrogen-bond acceptor at the corresponding ligand position was considered to be crucial for binding
243 (Fig. 3). Further, in most of the structures the ligands formed interactions with Trp105 (*Ambler*
244 numbering) [22]. Therefore, this interaction was also included in the pharmacophore hypothesis.
245 Hydrogen-bond interactions to Asn130 were found in four structures (PDB codes 3RXW, 3G32, 3G30,
246 4EUZ) and included as well.

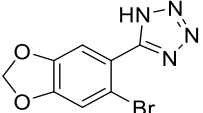
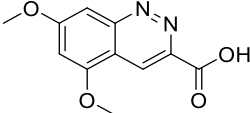
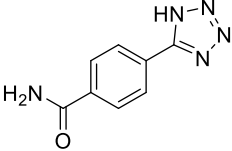
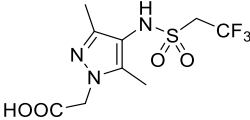
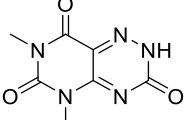
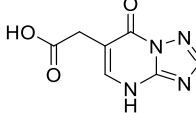
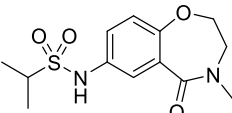
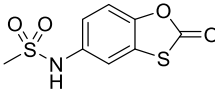
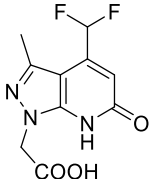
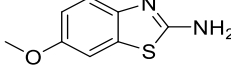
247

248 A hierarchical approach was adopted for virtual screening. First, our in-house database of around five
249 million purchasable compounds was filtered for lead-like molecules [23]. In the second step, the
250 obtained hits were screened with the above-described pharmacophore resulting in 44658 compounds.
251 Out of these, 31122 compounds could be docked into the *Kp* KPC2 binding site. Filtering these binding

252 poses again with the pharmacophore resulted in 2894 compounds. These were divided into three
253 clusters, depending on the functional group placed in the hydrophilic pocket (tetrazoles, carboxylates,
254 sulfonamides) and inspected by eye. Finally, 31 compounds were selected for hit validation (Table 2).
255 Most of the selected chemotypes carried an anionic group, mainly a carboxylic group or its bioisostere,
256 the tetrazole ring. Candidates were predicted to orient the anionic side of their moiety in the carboxylic
257 acid binding site of KPC-2, delimited by Ser130, Thr235 and Thr237 and present in all serine-based
258 Beta-lactamases. In the above mentioned site, in fact, binds the C(3)4' carboxylate of β -lactams
259 antibiotics as well as the sulfate group of avibactam and the carboxylic group of other known BLs
260 inhibitors [12,32,37,38,39].
261

Table 2. Inhibitory activity of compounds selected from virtual screening.

ID	Structure	IC ₅₀ mM ^[a,b]	ID	Structure	IC ₅₀ mM ^[a,b]
1a		> 0.33 (30)	17a		>1.0 (23)
2a		> 0.50 (38)	18a		1.0 (18)
3a		>0.25 (13)	19a		0.88
4a		>0.25 (12)	20a ^[c]		>0.5 (28)
5a		>0.50 (13)	21a		>1.0 (12)
6a		>1.0 (18)	22a		NI at 1.0
7a		>1.0 (12)	23a		>1.0 (26) ^[c]
8a		>0.50 (37)	24a		>0.1 (41)
9a ^[b]		0.15 ^[c]	25a		> 0.4 (26)
10a ^[b]		0.07 ^[c]	26a		> 0.83 (18)
11a ^[b]		0.036 ^[c]	27a		NI at 0.5

12a ^[b]		0.70 ^[c]	28a		>0.5 (14)
13a		NI at 0.25	29a		>1.0 (15)
14a		>1.0 (26)	30a		NI at 1.0
15a		>0.66 (38)	31a		>1.0 (11)
16a		>1.0 (17)	32a		1.24

^[a]Assays were performed in duplicate (errors were less than 5%) with CENTA as reporter substrate (100 μ M, km 70 μ M). Kinetic were monitored at 25° by following the absorbance variation at $\lambda = 405$ nm. ^[b] If no IC_{50} has been measured, percent inhibition at the highest tested concentration is given in parentheses. For example, > 0.50 (26 %) implies that the highest concentration tested was 0.50 mM; at this concentration, the enzyme was inhibited by 26 %. Therefore, $IC_{50} > 0.50$ mM. When % Inhibition was below 10% No Inhibition (NI) is reported in table. ^[c]Assays were run after 10' incubation of the inhibitor with KPC-2. Reaction was started by the addition of CENTA.

262

263 Hit Evaluation

264 The majority of the selected candidates were fragment-like as defined by the “rule of three” [14]. Thus,
 265 potencies in the high micromolar to millimolar range were expected. Unfortunately, the required high
 266 concentrations for ligand testing could not always be achieved due to solubility issues which might have
 267 resulted false negatives after testing. However, some of the tested molecules inhibited the hydrolytic
 268 activity of KPC-2 with millimolar potency. Among those, compounds **9a** and **11a** were the most
 269 promising compounds with micromolar affinities (IC_{50} of 0.15 and 0.036 mM, translating to ligand
 270 efficiencies (LE) of 0.38 and 0.28 kcal/mol/non-hydrogen atom, respectively; Table 2) and were thus
 271 further investigated.

272 Compound **9a** was predicted to place its carboxylate group in proximity of the catalytic Ser70, in the
 273 carboxylic acid binding site mentioned above, forming hydrogen bond interactions with the side chains
 274 corresponding to amino acids Ser130, Thr235 and Thr237 (Fig. 6). Thr 237 in KPC-2 is known to be

275 necessary for cephalosporinase and carbapenemase activity and is involved in clavulanic acid, sulbactam
276 and tazobactam recognition.[7] This position in β -lactamases that do not have carbapenemase or
277 extended-spectrum β -lactamase (ESBL) activity generally corresponds to an alanine. The side chain
278 hydroxyl groups of Ser130 and Ser70 were predicted to form interactions with the nitrogen of the
279 benzothiazole ring. The predicted position of the aromatic system is well placed to establish ring-ring
280 interactions with Trp105, a residue involved, in turn, in the stabilization of β -lactams through mainly
281 hydrophobic and van der Waals interactions (centroids distances of 4.4 and 4.5 Å between Trp105 and
282 the thiophene and the benzene rings respectively) The role of Trp105 in substrate and inhibitor
283 interactions in KPC-2 β -lactamase has been deeply investigated being essential for hydrolysis of
284 substrates.[7] The methoxy group of the molecule is oriented towards a rather open and solvent
285 accessible area of the binding site and does not contact any of the surrounding residues. Interestingly,
286 the presence of the sulphur atom of the benzothiazole system seems critical for affinity as the related
287 compound **19a**, the benzimidazole analog, resulted 6-fold less active. Similar, the presence of the
288 carboxylic group appeared to be crucial as compound **32a**, without such a functionality, was 8-fold less
289 active.

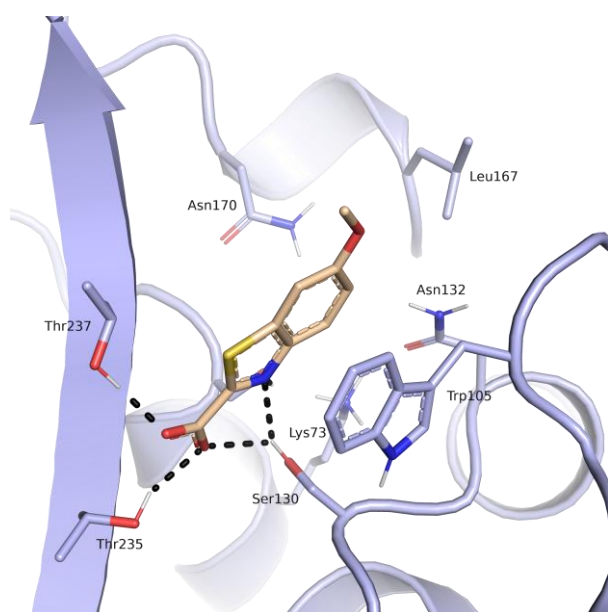


Figure 6. Predicted binding mode of compound **9a** (beige) in the *KpKPC-2* receptor (blue). Putative hydrogen bond interactions are indicated as black dots (Ambler numbering)[22].

290

291 For compound **9a** binding affinity and mode of inhibition was determined by using gradient

292 concentrations of CENTA. Fitting of the obtained data showed that compound **9a** behaves as a
293 competitive inhibitor with a determined K_i of 112.0 μM (Fig. 7). Its binding affinity was also determined
294 towards other class A β -lactamases (IC_{50} vs CTX-M9 160 μM). For this compound aggregating behavior
295 was also excluded by dynamic light scattering experiment (data not shown) [40]. Compound **9a** with its
296 fragment-like characteristic (MW 208.21, determined K_i 112.0 μM , LE 0.38 kcal/mol/non-hydrogen
297 atom) exerts an interesting activity vs KPC2-2 and represents a very promising molecule to be directed
298 to hit to lead optimization.

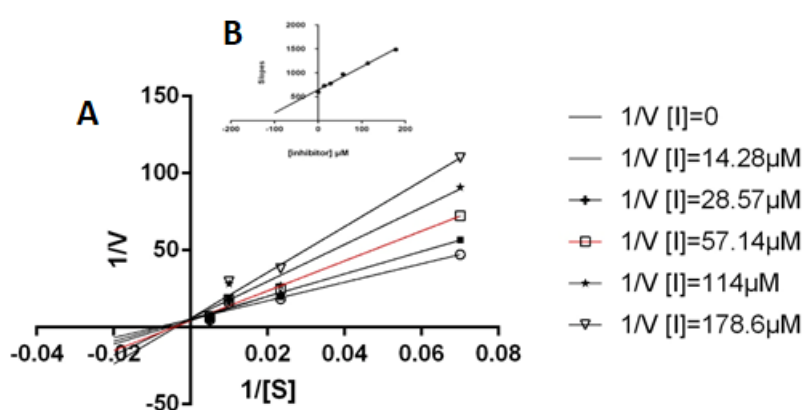


Figure 7. (A) Lineweaver–Burk plot (A) and Dixon slope plot (B) for competitive inhibitor, compound **9a**.

299
300 Among the 32 selected hits evaluated *in vitro* for their binding affinity vs KPC-2, compound **11a** was
301 the most active inhibitor with a micromolar affinity vs KPC-2 (determined IC_{50} 36 μM , calculated K_i
302 14.8 μM , LE 0.28 kcal/mol/non-hydrogen atom).[36] The tetrazole ring of compound **11a**, a well-known
303 bioisostere of the carboxylic group, was predicted to lie in the hydrophilic pocket formed by Thr235,
304 Thr237, Ser130 and Ser70, driving the binding of the inhibitor in KPC-2 active site(Fig. 8). The phenyl
305 ring attached to the tetrazole was predicted to be sandwiched between the Trp105 side with a distance
306 compatible with weak hydrophobic interactions and the backbone of Thr237. The amide group of **11a**
307 was oriented in the canonical site delimited by Asn132, Asn170 and in a further distance Glu166 where
308 the R1 amide side chain of β -lactams is known to bind. However, the amine linker and the second phenyl
309 ring in **11a** were not predicted to form any specific interactions with the protein, except for the amide

310 nitrogen contacting the backbone of Thr237. The distal fluoro-benzene ring was oriented at the entrance
311 of the active site against two hydrophobic patches, one defined by Leu167, closer, and the other by the
312 backbone of Asn170, a residue critical for carbapenemase activity.

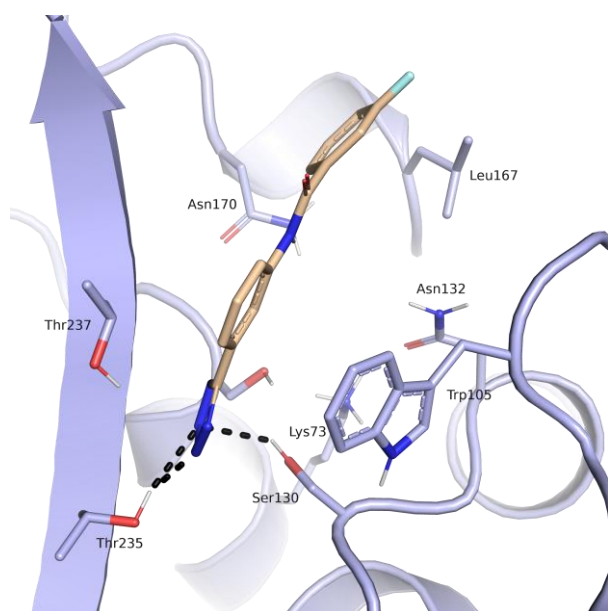


Figure 8. Predicted binding mode of compound **11a** (beige) in the *KpKPC-2* receptor (blue). Putative hydrogen bond interactions are indicated as black dots (Ambler numbering)[22].

313
314 Based on the predicted binding mode, the tetrazole group of **11a** seemed to be crucial for affinity. (Table
315 1). Moreover, while the proximal ring appeared to be involved in specific interactions, the amide group
316 and the distal ring did not contact efficaciously the protein. Based on predicted binding mode, chemical
317 size, synthetic accessibility for a rapid structural optimization and ligand efficacy compound **11a** was
318 directed to chemical synthesis development to improve its affinity and to investigate target binding
319 requirements for optimal inhibitor-enzyme interaction.

320 **Hit derivatization and evaluation**

321 In order to improve the binding affinity of **11a**, the compound was subjected to a hit optimization
322 program. Therefore, the phenyl-tetrazole moiety, that seemed to strongly drive the binding, was retained
323 unaltered, whereas structural modifications on the linker and on the distal aromatic ring were introduced

324 in order to explore and maximize the interactions with the pocket formed by Asn132, Asn170 and
325 Leu167 (Fig. 6). Because the amide linker does not contact efficaciously the protein we chose to replace
326 it with a sulfonamide (Fig. 9). We meant to target residues proximal to the opening of the active site
327 while investigating the potentiality for sulfonamide derivatives.
328

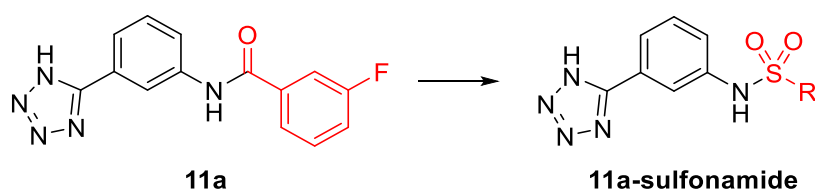


Figure 9. Virtual Screening hit **11a** (left), amine 1 (black) and the optimized part of the molecule (red).

329
330 Sulfonamides are more stable towards hydrolysis than carboxyamides, possess an additional hydrogen
331 bonding oxygen atom and their NH is a strong hydrogen bond donor. In addition, the dihedral angle ' ω '
332 OSNH measures around 90° compared with the 180° ' ω ' OCNH angle of amide. Sulfonamides, in
333 addition, have a non-planar configuration that could orient the distal ring towards Leu167 and Asn170
334 (Fig. 10). Therefore, the introduction of a sp^3 geometry could allow a more efficacious spanning of the
335 active site compared to the planar amide [41]. Moreover, modeling suggested that the sulfonamide group
336 could form an additional hydrogen bond with Asn132 residue actively involved in substrate recognition
337 and hydrolysis.
338
339

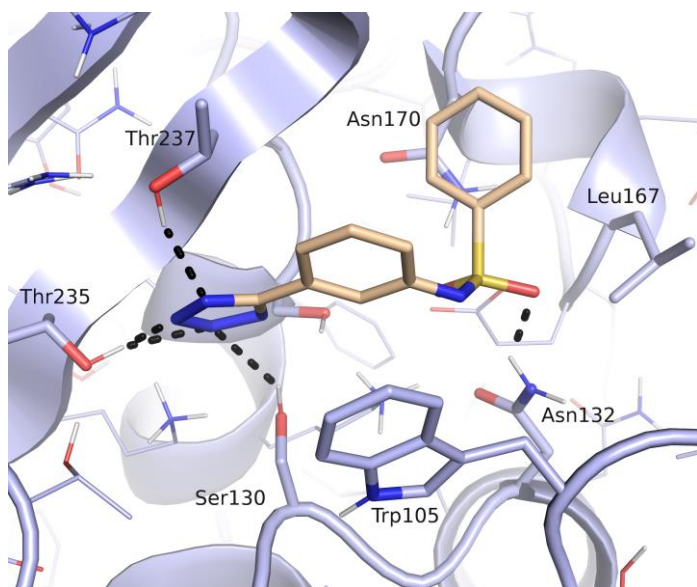
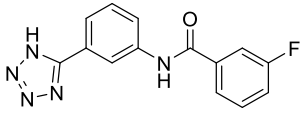
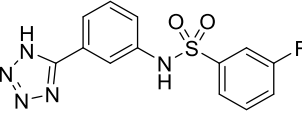
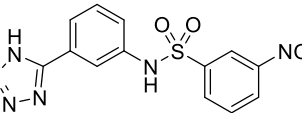
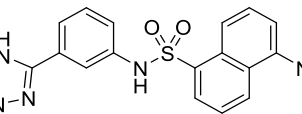
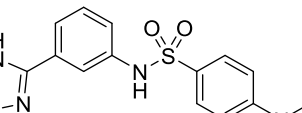
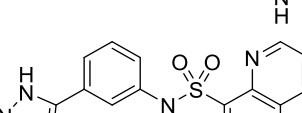
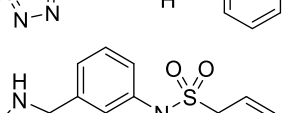
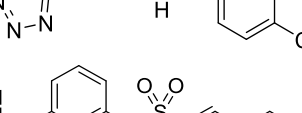
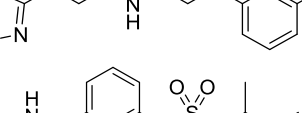
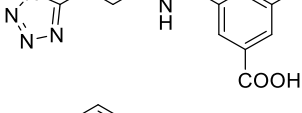
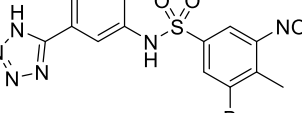


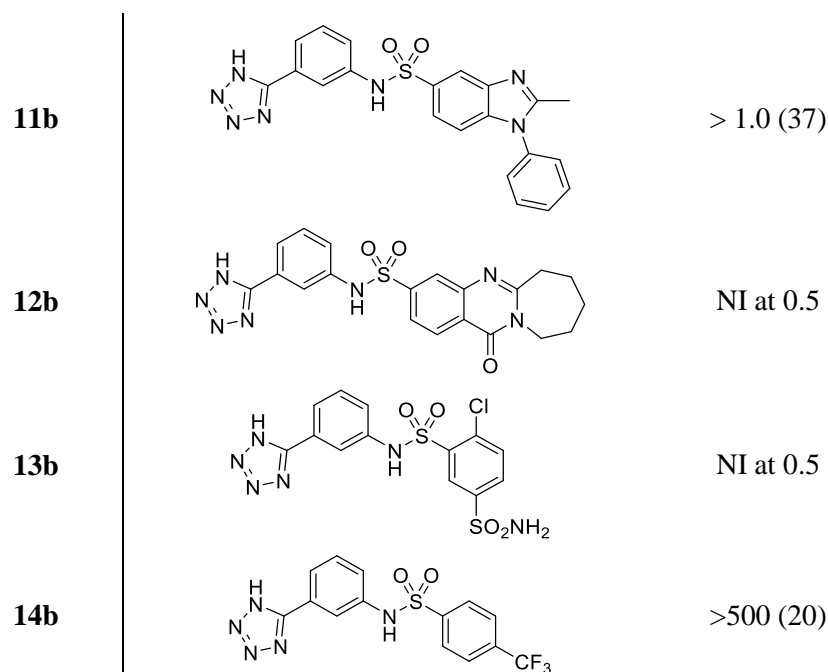
Figure 10. Predicted binding mode of a sulfonamide derivative of compound **11a** (beige) in the *KpKPC-2* receptor (blue). Putative hydrogen bond interactions are indicated as black dots (Ambler numbering)[22].

340 Further, we explored different substitutions on the sulfonamide linker to probe binding interactions.
341 Substituents with different electronic and steric properties (i.e. halogens, nitro, sulfonamide, carboxylic
342 acid, methyl, acetamide, amino groups) were inserted in the different position of the aromatic ring. In
343 addition, the benzene ring was replaced by heterocyclic or extended benzofused systems such as
344 benzimidazole, quinazolinone, naphthalene, or quinolone ring. Based on the availability of compound
345 or building blocks, 6 compounds (**1b-6b**) were synthesized and 8 compounds (**7b-14b**) were purchased
346 to test our hypothesis (Table 3). The fourteen new compounds were tested *in vivo* vs clinical strains
347 overproducing KPC-2 to evaluate their ability to restore bacteria susceptibility to carbapenem
348 meropenem (Table 4).

349

Table 3: Inhibitory activity of **11a** sulphonamide derivatives.

ID	STRUCTURE	IC ₅₀ mM ^[a,b]
11a		0.036
1b		> 0.2 (25)
2b		>0.6 (23)
3b		Not tested not soluble
4b		> 0.2 (16)
5b		> 0.2 (13)
6b		NI at 0.2
7b		>1.0 (30)
8b		> 1.0 (37)
9b		NI at 0.5
10b		NI at 0.5

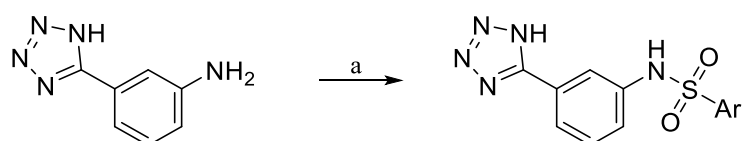


350 ^[a]Assays were performed in duplicate (errors were less than 5%) with nitrocefin (114.28 μ M, K_m 36 μ M) as
 351 reporter substrate Kinetic were monitored at 25° by following the absorbance variation at $\lambda = 485$ nm. ^[b] If no IC_{50}
 352 has been measured, percent inhibition at the highest tested concentration is given in parentheses. For example, >
 353 1.0 (37 %) implies that the highest concentration tested was 1.0 mM; at this concentration, the enzyme was
 354 inhibited by 37 % and $IC_{50} > 1.0$ mM. When % Inhibition was below 10% No Inhibition (NI) is reported in table.
 355

356

357 Compounds **1b-6b** were synthesized in high yield (75-95% yield) and purity (>95%) through direct
 358 reaction of 3-(1H-tetrazol-5-yl) aniline and the appropriate sulfonyl chloride in dichloromethane at room
 359 temperature for 3 hours (Fig. 11).

360



1b Ar: 3-F-C₆H₄-
2b Ar: 3-NO₂-C₆H₄-
3b Ar: Dansyl-
4b Ar: 4-(CH₃CONH-)C₆H₄-
5b Ar: 8-Quinoline-
6b Ar: 4-Cl-C₆H₄-

Figure 11. Reagents and conditions. a) aryl-sulfonyl chloride (1.2 eq.), pyridine (3 eq.), dry DCM, N₂, r.t, 3 h, 75-95% yield.

361 The derivatives of compound **11a** were tested for KPC-2 affinity (Table 3). They exhibited either weaker
 362 activities than **11a** or were not active at all at tested concentration. Thus, it appeared that the sulfonamide
 363 linker is not a suitable group to optimize the affinity of this compound series.

364
 365 The antimicrobial activity of the best hits **9a** and **11a** and their derivatives was studied in bacterial cell
 366 cultures to investigate their ability to cross the outer membrane reaching the periplasmic space, where
 367 KPC-2 is secreted and confined in Gram negative bacteria. Compounds were tested for synergy with the
 368 β -lactam antibiotic meropenem against four *K. pneumoniae* clinical strains, isolated from different
 369 patients at the Hospital Universitario Son Espases, Palma de Mallorca, Spain. One of the four clinical
 370 strains was not a KPC-2 producer and was susceptible to meropenem (strain **Kpn (C-)**; MIC <0.25
 371 μ g/mL). The three additional strains harbored the blaKPC-2 gene and were resistant to meropenem
 372 (Table 4). [32] Noteworthy none of the tested compounds had intrinsic antibiotic activity (MIC >256
 373 μ g/mL), against the employed strains, included the susceptible one. The results show that in most cases
 374 the compounds were not able to reverse antibiotic resistance and did not showed synergism with
 375 meropenem. However, against strain Kpn 53A8 the MIC value was lowered by a factor of two when
 376 meropenem was combined with compounds **32a**, **1b**, **2b**, **5b** and **6b** while in combination with
 377 compound **11a** the MIC value was reduced by 4 fold.

378
 379 **Table 4:** *In vitro* interaction between meropenem and synthesized compounds vs *K. pneumoniae*
 380 clinical strains.

MIC ^[a] meropenem in combination with synthesized compounds (1:1 molar) ^[a, b, c] (μ g/mL)				
Code	Kpn (C-)	Kpn 99D8	Kpn 53A8	Kpn 53A9
--	<0.25	256	256	256
9a	<0.25	256	256	256
11a	<0.25	256	64	256
32a	<0.25	256	128	256
1b	<0.25	256	128	256
2b	<0.25	256	128	256
4b	<0.25	256	256	256
5b	<0.25	256	128	256
6b	<0.25	256	128	256

381 ^[a] Assays were conducted against four *K. pneumoniae* clinical strains isolated from different patients at the
 382 Hospital Universitario Son Espases, Palma de Mallorca, Spain. MICs were determined according to EUCAST
 383 standards and the presented values are the median of three independent experiments.

384 ^[b] Compounds were testes alone and showed no activity (MIC>256) in all cases.

385 ^[c] Strain C- is control *K. pneumoniae* and meropenem susceptible (MIC < 0.25 μ g/ml)

386 **Conclusions**

387 In this study two novel KPC-2 inhibitors were identified via an *in-silico* approach. 14 novel tetrazole
388 derivatives originating from the best, low micromolar, hit **11a** were designed, synthesized and evaluated
389 for their ability to inhibit KPC-2. We introduced chemical diversity on the distal part of the inhibitor,
390 choosing to keep unchanged the anchor tetrazole ring while modifying the amide and the distal ring.
391 The results suggests that a sulfonamide linker is not suitable to improve the potency of **11a**. Future
392 optimization work should instead rather concentrate on exploring secondary binding sites more distal
393 from the pocket that the screening hits are supposed to address [42]. If the amide functionally found in
394 **11a** or alternative linkers are best suited remains to be explored. Nevertheless, two promising hit
395 compounds for KPC-2 were retrieved which can serve as starting points to derive more potent inhibitors.
396 Although a decrease of potency in *in vitro* tests was registered for the designed and synthesized chemical
397 entities, as none of the compounds was able to trigger stronger interactions with the open region of KPC-
398 2 they were meant to target, this study yielded a better comprehension of the catalytic pocket of this
399 enzyme. Our study provided a better understanding of how challenging the target of additional,
400 superficial, binding pockets is and how it could be critical in designing inhibitors with improved
401 potency, especially in area proximal to the active site opening.

402 The (1H-tetrazol-5-yl)phenyl ring was most frequents among the high scoring candidates in our *in silico*
403 study, suggesting that this functionality is well suited to anchor ligands in the in KPC-2 binding site.
404 The rather weak affinity of the ligands hints that rest of the ligand, i.e. the functional groups out of the
405 center phenyl ring and the amide liker, need to be optimized to increase potency. However, introducing
406 a sulfonamide linker was detrimental for potency. We hypothesize that the presence of a sulfonamide
407 instead of an amide led to a rearrangement of the ligand in the binding site to minimize steric hindrance,
408 and thus resulted in the loss of key interactions. These rearrangements can be particularly critical in non-
409 covalent inhibitors like ours that are not stabilized by a covalent interaction with the catalytic serine, as
410 this type of inhibitors are supposed to have lower residence times with respect to covalent β -lactamase
411 inhibitors (Fig.1). In designing larger and more potent inhibitors, additional secondary binding sites
412 which have been found to be critical for affinity improvement need to be considered [42]. Further

413 medicinal chemistry work is ongoing to significantly increase the potency of the most promising
414 compound **11a** *in vitro* and *in vivo* and new chemistry is under evaluation for these derivatives, taking
415 advantage of other additional recognition sites in KPC-2.

416

417 **Acknowledgements**

418 We thank Hayarpi Torosyan from Brian K Shoichet's Laboratory at USCF for dynamic light scattering
419 measurements on compound **9a**, Josef Kehrein for contributions to the modelling work, and Openeye
420 for free software licenses. Virtual screening was performed on resources provided by UNINETT Sigma2
421 - the National Infrastructure for High Performance Computing and Data Storage in Norway and the
422 Mogon cluster of the Johannes Gutenberg University Mainz.

423 **Funding**

424 The project was funded by Fondo di Ricerca di Ateneo UNIMORE to DT. The funder played no role in
425 the conducted research.

426 **References**

- 427 1. Papp-Wallace KM, Endimiani A, Taracila MA, Bonomo RA. Carbapenems: Past, present, and
428 future. *Antimicrob Agents Chemother.* 2011;55: 4943–4960. doi:10.1128/AAC.00296-11
- 429 2. Tondi D, Cross S, Venturelli A, Costi MP, Cruciani G, Spyraakis F. Decoding the Structural
430 Basis For Carbapenem Hydrolysis By Class A beta-lactamases: Fishing For A Pharmacophore.
431 *Curr Drug Targets.* Netherlands; 2016;17: 983–1005.
- 432 3. Livermore DM, Woodford N. The beta-lactamase threat in Enterobacteriaceae, Pseudomonas
433 and Acinetobacter. *Trends Microbiol.* England; 2006;14: 413–420.
434 doi:10.1016/j.tim.2006.07.008
- 435 4. Farina D, Spyraakis F, Venturelli A, Cross S, Tondi D, Paola Costi M. The Inhibition of
436 Extended Spectrum β -Lactamases: Hits and Leads. *Current Medicinal Chemistry.* 2014; 21:
437 1405–1434
- 438 5. Frère J-M, Sauvage E, Kerff F. From “An Enzyme Able to Destroy Penicillin” to

- 439 Carbapenemases: 70 Years of Beta-lactamase Misbehaviour. *Current Drug Targets*. 2016;17:
440 974–982
- 441 6. Naas T, Dortet L, I. Iorga B. Structural and Functional Aspects of Class A Carbapenemases.
442 *Current Drug Targets*. 2016;17: 1006–1028.
- 443 7. Papp-Wallace KM, Bethel CR, Distler AM, Kasuboski C, Taracila M, Bonomo RA. Inhibitor
444 resistance in the KPC-2 beta-lactamase, a preeminent property of this class A beta-lactamase.
445 *Antimicrob Agents Chemother*. United States; 2010;54: 890–897. doi:10.1128/AAC.00693-09
- 446 8. Brem J, Cain R, Cahill S, McDonough MA, Clifton IJ, Jiménez-Castellanos J-C, et al.
447 Structural basis of metallo- β -lactamase, serine- β -lactamase and penicillin-binding protein
448 inhibition by cyclic boronates. *Nat Commun*. 2016;8: 12406.
- 449 9. Santucci M, Spyraakis F, Cross S, Quotadamo A, Farina D, Tondi D, et al. Computational and
450 biological profile of boronic acids for the detection of bacterial serine- and metallo- β -
451 lactamases. *Sci Rep*. 2017;7: 1–15. doi:10.1038/s41598-017-17399-7
- 452 10. Danishuddin M, Khan AU. Structure based virtual screening to discover putative drug
453 candidates: Necessary considerations and successful case studies. *Methods*. 2015;71: 135–145.
454 doi:<https://doi.org/10.1016/j.ymeth.2014.10.019>
- 455 11. Khan A, Faheem M, Danishuddin M, Khan AU. Evaluation of Inhibitory Action of Novel Non
456 β -Lactam Inhibitor against *Klebsiella pneumoniae* Carbapenemase (KPC-2). *PLoS One*.
457 2014;9: e108246.
- 458 12. Krishnan NP, Nguyen NQ, Papp-Wallace KM, Bonomo RA, van den Akker F. Inhibition of
459 *Klebsiella* β -Lactamases (SHV-1 and KPC-2) by Avibactam: A Structural Study. *PLoS One*.
460 2015;10: e0136813.
- 461 13. Pemberton OA, Zhang X, Chen Y. Molecular Basis of Substrate Recognition and Product
462 Release by the *Klebsiella pneumoniae* Carbapenemase (KPC-2). *J Med Chem*. 2017;60: 3525–
463 3530. doi:10.1021/acs.jmedchem.7b00158
- 464 14. Congreve M, Carr R, Murray C, Jhoti H. A “rule of three” for fragment-based lead discovery?
465 *Drug Discov Today*. 2003;8: 876–877.
- 466 15. Ito JI, Tabei Y, Shimizu K, Tsuda K, Tomii K. PoSSuM: A database of similar protein-ligand

- 467 binding and putative pockets. *Nucleic Acids Res.* 2012;40: 541–548. doi:10.1093/nar/gkr1130
- 468 16. Ito JI, Ikeda K, Yamada K, Mizuguchi K, Tomii K. PoSSuM v.2.0: Data update and a new
469 function for investigating ligand analogs and target proteins of small-molecule drugs. *Nucleic*
470 *Acids Res.* 2015;43: D392–D398. doi:10.1093/nar/gku1144
- 471 17. Ke W, Bethel CR, Papp-Wallace KM, Pagadala SRR, Nottingham M, Fernandez D, et al.
472 Crystal structures of KPC-2 beta-lactamase in complex with 3-nitrophenyl boronic acid and
473 the penam sulfone PSR-3-226. *Antimicrob Agents Chemother.* 2012;56: 2713–2718.
474 doi:10.1128/AAC.06099-11
- 475 18. Nichols DA, Jaishankar P, Larson W, Smith E, Liu G, Beyrouthy R, et al. Structure-based
476 design of potent and ligand-efficient inhibitors of CTX-M class A β -lactamase. *J Med Chem.*
477 2012;55: 2163–2172. doi:10.1021/jm2014138
- 478 19. Tomanicek SJ, Standaert RF, Weiss KL, Ostermann A, Schrader TE, Ng JD, et al. Neutron and
479 X-ray Crystal Structures of a Perdeuterated Enzyme Inhibitor Complex Reveal the Catalytic
480 Proton Network of the Toho-1 β -Lactamase for the Acylation Reaction. *J Biol Chem.* 2013;15:
481 4715-4722
- 482 20. Chen Y, Shoichet BK. Molecular docking and ligand specificity in fragment-based inhibitor
483 discovery. *Nat Chem Biol.* 2009;5: 358–364. doi:10.1038/nchembio.155
- 484 21. Fonseca F, Chudyk EI, van der Kamp MW, Correia A, Mulholland AJ, Spencer J. The Basis
485 for Carbapenem Hydrolysis by Class A β -Lactamases: A Combined Investigation using
486 Crystallography and Simulations. *J Am Chem Soc. American Chemical Society;* 2012;134:
487 18275–18285. doi:10.1021/ja304460j
- 488 22. Ambler RP, Coulson AF, Frere JM, Ghuysen JM, Joris B, Forsman M, et al. A standard
489 numbering scheme for the class A beta-lactamases. *The Biochemical journal.* England;
490 1991;15: 269–270.
- 491 23. Brenk R, Schipani A, James D, Krasowski A, Gilbert IH, Frearson J, et al. Lessons learnt from
492 assembling screening libraries for drug discovery for neglected diseases. *ChemMedChem.*
493 2008;3: 435–444. doi:10.1002/cmdc.200700139
- 494 24. Hawkins PCD, Skillman AG, Warren GL, Ellingson BA, Stahl MT. Conformer Generation

- 495 with OMEGA: Algorithm and Validation Using High Quality Structures from the Protein
496 Databank and Cambridge Structural Database. *J Chem Inf Model.* 2010;50: 572–584.
497 doi:10.1021/ci100031x
- 498 25. Mpamhanga CP, Spinks D, Tulloch LB, Shanks EJ, Robinson DA, Collie IT, et al. One
499 scaffold, three binding modes: Novel and selective pteridine reductase 1 inhibitors derived
500 from fragment hits discovered by virtual screening. *J Med Chem.* 2009;52: 4454–4465.
501 doi:10.1021/jm900414x
- 502 26. Brenk R, Irwin JJ, Shoichet BK. Here Be Dragons: Docking and Screening in an Uncharted
503 Region of Chemical Space. *J Biomol Screen.* 2005;10: 667–674.
504 doi:10.1177/1087057105281047
- 505 27. Mysinger MM, Shoichet BK. Rapid context-dependent ligand desolvation in molecular
506 docking. *J Chem Inf Model.* 2010;50: 1561–1573. doi:10.1021/ci100214a
- 507 28. Lorber DM, Shoichet BK. Flexible ligand docking using conformational ensembles. *Protein*
508 *Sci.* 1998;7: 938–950.
- 509 29. Wei BQ, Baase WA, Weaver LH, Matthews BW, Shoichet BK. A Model Binding Site for
510 Testing Scoring Functions in Molecular Docking. *J Mol Biol.* 2002;322: 339–355.
511 doi:10.1016/S0022-2836(02)00777-5
- 512 30. Kuntz ID, Chen K, Sharp KA, Kollman PA. The maximal affinity of ligands. *Proc Natl Acad*
513 *Sci.* 1999;96: 9997–10002.
- 514 31. Hopkins AL, Groom CR, Alex A. Ligand efficiency : a useful metric for lead selection. *Drug*
515 *Discov Today.* 2004;9: 430–431.
- 516 32. Celenza G, Vicario M, Bellio P, Linciano P, Perilli M, Oliver A, et al. Phenylboronic Acid
517 Derivatives as Validated Leads Active in Clinical Strains Overexpressing KPC-2: A Step
518 against Bacterial Resistance. *ChemMedChem.* 2018; doi:10.1002/cmdc.201700788
- 519 33. Crompton R, Williams H, Ansell D, Campbell L, Holden K, Cruickshank S, et al. Oestrogen
520 promotes healing in a bacterial LPS model of delayed cutaneous wound repair. *Lab Invest.*
521 *United States;* 2016;96: 439–449. doi:10.1038/labinvest.2015.160
- 522 34. Feng BY, Shoichet BK. A detergent-based assay for the detection of promiscuous inhibitors.

- 523 Nat Protoc. 2006;1: 550–553. doi:10.1038/nprot.2006.77
- 524 35. Quotadamo A, Linciano P, Davoli P, Tondi D, Costi MP, Venturelli A. An Improved Synthesis
525 of CENTA, a Chromogenic Substrate for β -Lactamases. *Synlett*. 2016;27: 2447–2450.
526 doi:10.1055/s-0035-1562454
- 527 36. Cheng Y, Prusoff WH. Relationship between the inhibition constant (K₁) and the concentration
528 of inhibitor which causes 50 per cent inhibition (I₅₀) of an enzymatic reaction. *Biochem*
529 *Pharmacol*. England; 1973;22: 3099–3108.
- 530 37. Strynadka NC, Adachi H, Jensen SE, Johns K, Sielecki A, Betzel C, et al. Molecular structure
531 of the acyl-enzyme intermediate in beta-lactam hydrolysis at 1.7 Å resolution. *Nature*.
532 1992;359: 700–705. doi:10.1038/359700a0
- 533 38. Tondi D, Venturelli A, Bonnet R, Pozzi C, Shoichet BK, Costi MP. Targeting class A and C
534 serine beta-lactamases with a broad-spectrum boronic acid derivative. *J Med Chem*.2014;57:
535 5449–5458. doi:10.1021/jm5006572
- 536 39. Genovese F, Lazzari S, Venturi E, et al (2017) Design, synthesis and biological evaluation of
537 non-covalent AmpC β -lactamases inhibitors. *Med Chem Res* 26:975–986 . doi:
538 10.1007/s00044-017-1809-x
- 539 40. Seidler J, McGovern SL, Doman TN, Shoichet BK. Identification and Prediction of
540 Promiscuous Aggregating Inhibitors among Known Drugs. *J Med Chem*. 2003;46: 4477–4486.
541 doi:10.1021/jm030191r
- 542 41. Vijayadas KN, Davis HC, Kotmale AS, Gawade RL, Puranik VG, Rajamohanan PR, et al. An
543 unusual conformational similarity of two peptide folds featuring sulfonamide and carboxamide
544 on the backbone. *Chem Commun*. The Royal Society of Chemistry; 2012;48: 9747–9749.
545 doi:10.1039/C2CC34533A
- 546 42. Babaoglu K, Shoichet BK. Deconstructing fragment-based inhibitor discovery. *Nature*
547 *chemical biology*.2006;2: 720–723. doi:10.1038/nchembio831
- 548